Catalysis

DOI: 10.1002/ange.201310097

Activation of Oxygen on Gold and Silver Nanoparticles Assisted by Surface Plasmon Resonances**

Yi-Fan Huang, Meng Zhang, Liu-Bin Zhao, Jia-Min Feng, De-Yin Wu, Bin Ren,* and Zhong-Qun Tian*

Abstract: *Surface plasmon resonances (SPRs) have been found to promote chemical reactions. In most oxidative chemical reactions oxygen molecules participate and understanding of the activation mechanism of oxygen molecules is highly important. For this purpose, we applied surface-enhanced Raman spectroscopy (SERS) to find out the mechanism of SPR-assisted activation of oxygen, by using p-aminothiophenol (PATP), which undergoes a SPR-assisted selective oxidation, as a probe molecule. In this way, SPR has the dual function of activating the chemical reaction and enhancing the Raman signal of surface species. Both experiments and DFT calculations reveal that oxygen molecules were activated by accepting an electron from a metal nanoparticle under the excitation of SPR to form a strongly adsorbed oxygen molecule anion. The anion was then transformed to Au or Ag oxides or hydroxides on the surface to oxidize the surface species, which was also supported by the heating effect of the SPR. This work points to a promising new era of SPR-assisted catalytic reactions.*

The surface plasmon resonance (SPR) is an inherent oscillation of free-like electrons on material surfaces excited by incident photons, which results in the enhanced absorption and scattering of nanoparticles conferring rich color to nanomaterials, especially to gold, silver, and copper nanostructures. These unique properties are the reason for the wide application of SPR in enhanced spectroscopies (including Raman scattering, infrared absorption, second harmonic generation, and fluorescence) and thermotherapy.[1] More recently, it was found that SPR facilitated some chemical reactions.[2] For example, the epoxidation of ethylene and the splitting of water could be driven by sunlight on Ag and Au nanoparticles, respectively.[2c,f,h] It was reported about the dissociation of hydrogen on Au nanoparticles by illumination of laser light.[2g] If the dissociation of triplet oxygen molecules ($^3O_2$) could be also facilitated by SPR, it would significantly transform the field of catalytic reactions, as most oxidative chemical reactions involve the participation of oxygen molecules.

Recently, it was reported that $^3O_2$ can be sensitized to the singlet state ($^1O_2$) on Au, Ag, and Pt nanoparticles by illumination of visible laser light, which implies an interaction among light, nanoparticles, and $^3O_2$.[3] However, all the reports on SPR-assisted reactions were probed by ex situ or indirect techniques.[2] It is desired to develop methods to in situ trace the elementary steps of SPR-assisted activation of $^3O_2$ on the surface. Surface-enhanced Raman scattering (SERS) also originates from SPR with an ultrahigh sensitivity up to single-molecule level.[4] The same origin of SERS and SPR-assisted reaction endows SERS the power to provide in situ fingerprints of surface species during SPR-assisted reactions. SERS of $^3O_2$ adsorbed on the Ag film in the form of peroxidic and superoxidic dioxygen was studied.[5] Nonetheless, the adsorption of $^3O_2$ on metal surfaces is weak and was measured in ultrahigh vacuum at temperatures below −100 °C.

There are already several reports on laser-induced chemical transformation during SERS measurements.[6] Recently, we found that *p*-aminothiophenol (PATP) could be selectively and rapidly (in several seconds) oxidized to *p*,*p*′-dimercaptoazobenzene (DMAB) on Au or Ag nanoparticles at room temperature during conventional SERS measurements.[6e,g] Because the Raman measurement is performed in air, PATP may be selectively oxidized to DMAB by activated $^3O_2$ in the presence of SPR, as described in Equation (1).

$$2\,\mathrm{AuS{-}Ph{-}NH_2} + {}^3O_2 + h\nu \rightarrow \mathrm{AuS{-}Ph{-}N{=}N{-}Ph{-}SAu} + 2\,H_2O \quad (1)$$

Especially, a very recent work indicates the production of DMAB is associated with the presence of $^3O_2$.[6k] Therefore, the strong and characteristic bands of the produced DMAB may be used as indicators to monitor the activation of $^3O_2$.

Here, we mainly relied on the SERS observation of the selective oxidation of PATP to explore the SPR-assisted activation of $^3O_2$ on Au and Ag nanostructures. Because the SPR-assisted oxidation of PATP is involved in the interactions among light, $^3O_2$, PATP, and the surfaces, we first investigated the activation of $^3O_2$ by illumination of laser light and correlated it to the chemical properties of Au and Ag. Then, we characterized the surface species involved in the oxidation

[*] Dr. Y. F. Huang, M. Zhang, L. B. Zhao, Dr. J. M. Feng, Prof. Dr. D. Y. Wu, Prof. Dr. B. Ren, Prof. Dr. Z. Q. Tian
State Key Laboratory of Physical Chemistry of Solid Surfaces and Department of Chemistry
MOE laboratory of Spectrochemical Analysis and Instrumentation
Collaborative Innovation Center of Chemistry for Energy Materials
College of Chemistry and Chemical Engineering
Xiamen University, Xiamen 361005 (China)
E-mail: dywu@xmu.edu.cn
bren@xmu.edu.cn
Homepage: http://bren.xmu.edu.cn

[**] The project was supported by MOST (grant numbers 2013CB933703 and 2011YQ03012400) and NSFC (grant numbers 21227004, 21321062, 21373172, and 21021120456).

Supporting information for this article is available on the WWW under http://dx.doi.org/10.1002/anie.201310097.

of PATP to figure out the intermediates or products during the activation of $^3O_2$. Finally, the wavelength-dependent study and the theoretical calculations were carried out to demonstrate the SPR-assisted activation of $^3O_2$.

The role of $^3O_2$ activation during the production of DMAB was investigated by SERS measurement of PATP in an environment free of $^3O_2$. For this purpose, we prepared and sealed our samples in a glove box filled with N_2 where the concentration of $^3O_2$ and water is 0.4 and 0.01 ppm, respectively. To facilitate the diffusion and the reactions of $^3O_2$, the gap-mode SERS of the metal film/PATP/metallic nanoparticles (abbreviated as M film/PATP/M NPs) junctions were used, as depicted in Figure 1 a. The junctions were characterized by the SEM image shown in Figure 1 b (Au film/PATP/Au NPs) and precisely positioned in a Raman microscope equipped with the dark field function (see section S1 in the Supporting Information). The selective oxidation of PATP to DMAB by $^3O_2$ in the Au film/PATP/Au NPs can be clearly observed in illumination-time-dependent Raman spectra in air, shown in Figure 1 c.The bands at 1140, 1388, and 1434 cm^{-1} continuously increases with increasing illumination time. These bands can be assigned to the a_g modes of DMAB according to our previous work.[6f,i] Hence, the production of DMAB can be ascribed to the presence of $^3O_2$ shown by comparative Raman measurements of Au film/PATP/Au NPs in air and measurements in nitrogen (Figure 1 d). The a_g modes appear in the spectrum recorded in air but completely disappear in N_2 atmosphere. This observation indicates that $^3O_2$ in air would be first activated before the oxidation of PATP.

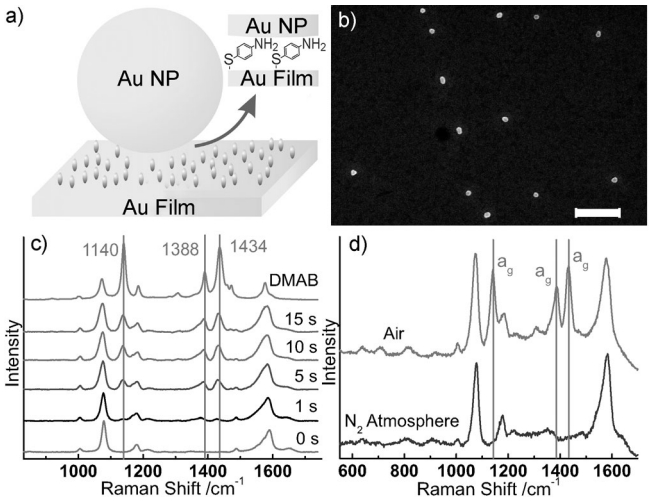

Figure 1. a) Au/PATP/Au nanoparticle, B) SEM image (the scale bar is 500 nm) and c) illumination-time-dependent Raman spectra and d) comparative Raman spectra of Au/PATP/Au NPs recorded in air and N_2 atmosphere.

The activation of $^3O_2$ on Au NPs can be evidenced by isolating Au NPs from $^3O_2$ and PATP. Therefore, a thin and compact silica layer was coated over Au NPs to avoid the contact of Au with air. Meanwhile, we used an atomically flat Au(111) surface to replace the Au film aiming to avoid the contact of the amino group with the Au surface at some rough features of the Au film surface. Figure 2 a shows Raman spectra obtained from Au(111)/PATP/Au@SiO_2 NPs and Au(111)/PATP/Au NPs recorded in air. We did not detect any signal of the a_g mode of DMAB in Au(111)/PATP/Au@SiO_2 NPs. Hence, it can be concluded that PATP should be oxidized by the activated $^3O_2$ on the Au NPs. However, the a_g modes of DMAB can be still observed in the SERS spectra of Au film/PATP/Ag NPs and Ag film/PATP/Au NPs recorded in N_2 atmosphere. The former gives a stronger signal than the latter, as shown in Figure 2 b. The intensity of the a_g modes recorded in the N_2 atmosphere is obviously lower than that in air. It has already been proposed that there may be some oxygen containing products as a result of the activation of $^3O_2$ on the Ag NPs or Ag film.[5] The hypothesis of such species was verified by X-ray photoelectron spectroscopy (XPS). Figure 2 c presents narrow survey spectra of the oxygen element obtained on Ag film/PATP/Au NPs and Au film/PATP/Ag NPs. The broad peak at about 532 eV can be ascribed to the Ag oxide or hydroxide.[7] Therefore, the oxidation of PATP can still occur in Au film/PATP/Ag NPs and Ag film/PATP/Au NPs systems in the N_2 atmosphere, which can be ascribed to the presence of the Ag oxide/hydroxide produced during the construction of junctions in air before the Raman measurement.

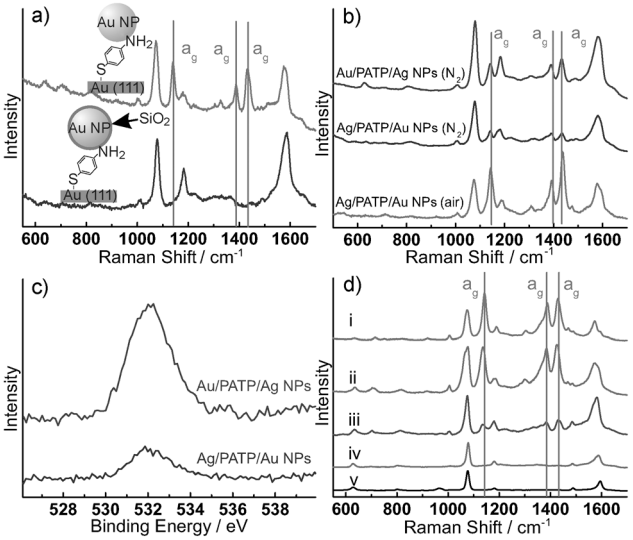

Figure 2. a) Raman spectra of Au(111)/PATP/Au NP (top) and Au(111)/PATP/Au@SiO_2 NP (bottom) junctions. b) Raman spectra of Ag film/PATP/Au NP and Au film/PATP/Ag NP junctions recorded in N_2 atmosphere and in air. c) XPS spectra of O-1s of Au/PATP/Ag NP and Ag/PATP/Au NP junctions. d) Raman spectra of PATP adsorbed on Ag NPs (i: 0.5 mol L^{-1} NaOH, iv: 0.5 mol L^{-1} H_2SO_4) and Au NPs (ii: 0.5 mol L^{-1} NaOH, iii: 0.5 mol L^{-1} H_2SO_4, v: 1.0 mol L^{-1} HCl) in solution.

One may wonder whether the Au and Ag oxides or hydroxides are involved in the activation of $^3O_2$ on the Au and Ag surfaces under laser light illumination, and then further oxidize the adsorbed PATP on the surface. However, it is still not conclusive whether $^3O_2$ in air can be activated on the Ag and Au surfaces to form surface oxides/hydroxides. Up to now, there is still no report on the production of oxide/hydroxide species on Au in air at room temperature. The

hypothesis can be confirmed by a comparative SERS study in NaOH, H_2SO_4, and HCl solutions in air on considering the following points. $^3O_2$ dissolved in solutions could be activated by illumination of laser light, which may produce Au or Ag oxides/hydroxides. The oxides or hydroxides are stable in NaOH solutions, and will not be easily removed. In H_2SO_4 solution, the Au oxide/hydroxide is stable and the Ag oxide/hydroxide will be dissolved. In HCl solution, the Au oxide/hydroxide will be dissolved as well, because of the complexation of Au cations with Cl^- anions. Figure 2d presents the Raman spectra of PATP adsorbed on Au NPs and Ag NPs in 0.5 mol L^{-1} NaOH, 0.5 mol L^{-1} H_2SO_4, and 1.0 mol L^{-1} HCl solution. The a_g modes of DMAB are strong in the basic environment (i and ii). In 0.5 mol L^{-1} H_2SO_4 solution, the a_g modes completely disappear on Ag NPs (iv) but still appear on Au NPs (iii). In 1.0 mol L^{-1} HCl and on Au NPs, the a_g modes also disappear. The above result indicates that PATP in the junctions is indeed oxidized by $^3O_2$ by the formation of Au or Ag oxides/hydroxides to yield DMAB.

The key role played by the oxides/hydroxides can be verified by DFT calculations. The calculated thermodynamic energy of the oxidation of PATP by $^3O_2$ is over −60 kcal mol^{-1}, which indicates that the oxidation is highly spontaneous, irrespective of the exact pathway. However, the activation barriers of the oxidation of PATP by AuOH, AgOH, Au_2O, and Ag_2O are 14.9, 7.3, 22.1, and 9.5 kcal mol^{-1}, which are much lower than that by $^3O_2$ (33.4 kcal mol^{-1}). Especially, the intermediates of the oxidation using oxides/hydroxides and $^3O_2$ are adsorbed nitrene species and aniline radicals on Ag or Au surfaces, respectively. Therefore, the calculation clearly indicates that the oxidation of PATP by Au or Ag oxides/hydroxides should be energetically preferred and highly selective (see section S3 in the Supporting Information for more details).

Based on the above discussion, we propose successive steps of the activation of $^3O_2$ by illumination of laser light on Au or Ag NPs. $^3O_2$ is first activated on the surface of Au or Ag by illumination of laser light. Then, the activated $^3O_2$ produces surface Au or Ag oxides/hydroxides. Finally, the Au or Ag oxides/hydroxides selectively oxidize PATP to DMAB. In these steps, the photon is mainly involved in the activation of $^3O_2$. As a result, we concentrated on studying the SPR-assisted activation of $^3O_2$. The wavelength dependence is one of the most important characters of SPR. Our previous work has found that the oxidation of PATP depends on the laser power density.[8] Therefore, in the present wavelength-dependent SERS study on Au film/PATP/Au NP junctions, we used the same laser power density of 9.6×10^7 mW cm^{-2}. Figure 3a presents the Raman spectra of Au film/PATP/Au NP junctions excited by a laser of 532, 632.8, and 785 nm in air. The intensity of all the bands excited by 532 nm light is much weaker than that by the other wavelengths. The intensity of a_1 modes at about 1080 and 1600 cm^{-1} primarily depends on the enhancement because of the SPR and their intensity can be used to characterize the enhancement.[6f] For example, the intensity of the band at 1080 cm^{-1}, assigned to the a_1 mode of PATP and DMAB, decreases following the order of 632.8 nm > 785 nm > 532 nm, which is consistent with the experimental observation in SERS. To obtain a more quantitative relationship, we normalized the intensity of the a_1 peak (1080 cm^{-1}) using 532 nm light as reference. The normalized intensity of the a_1 peak excited by 532, 632.8, and 785 nm laser light is 1, 200, and 40, respectively. Because the a_g modes are the characteristic bands of DMAB, the intensity ratio of a_g modes to a_1 mode can be used to estimate the yield of DMAB. The relative intensity of the bands at approximately 1140 cm^{-1} to the 1080 cm^{-1} peak excited by 532, 632.8, and 785 nm laser light is about 0.03, 1 and 0.1, respectively. In our previous SERS study of DMAB, we also found a similar intensity ratio for excitation by 532, 632.8, and 785 nm laser light.[6f] According to these results, we can qualitatively determine the yield of DMAB in the order of 632.8 nm > 785 nm > 532 nm (If we consider the maximal absorption of DMAB is in the green region, the yield at 532 nm will be even lower). It is consistent with the order of enhancement. Therefore, it can be concluded that the selective oxidation of PATP is further facilitated by the assistance of SPR.

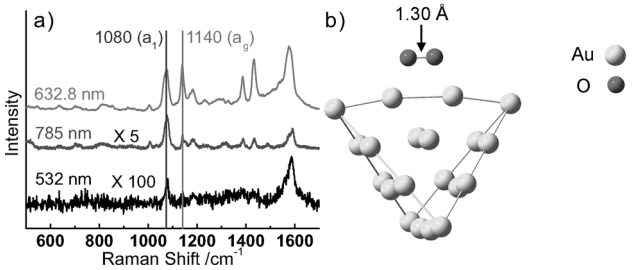

Figure 3. a) Wavelength-dependent Raman spectra of Au film/PATP/Au NP junctions excited using the same power density of 9.6×10^7 mW cm^{-2}. b) DFT-calculated geometry of Au_{20}-O_2^-.

In the above proposed activation scheme of $^3O_2$ and the wavelength-dependent transformation of PATP, we found that during oxidation of PATP to DMAB, the SPR-assisted activation of $^3O_2$ plays the most essential role. Recently, the SPR-assisted electron transfer from metal to $^3O_2$ has been proposed by the kinetic isotope effect on the reaction rate.[3c] Oxygen anions ($^2O_2^-$) are preferentially adsorbed on a metal surface compared with $^3O_2$, according to the experimental and theoretical calculations on small Au and Ag clusters containing up to 18 and 13 metallic atoms, respectively.[9] To understand the key step of our proposed mechanism, we performed DFT calculations of the adsorption of $^2O_2^-$ on Au_{20} and Ag_{20} clusters using a cluster model.[10] Figure 3b displays the geometrical structure of the Au_{20}-O_2^- cluster. The bond length of O–O is about 1.30 Å (1.32 Å in Ag_{20}-$^2O_2^-$), which is larger than that of free $^3O_2$ (about 1.21 Å). The adsorption free-energy of $^2O_2^-$ on Au_{20} and Ag_{20} is about −44.7 and −39.0 kcal mol^{-1}, respectively, indicating a strong adsorption of $^2O_2^-$. Therefore, we can conclude that $^3O_2$ can be activated on Au and Ag surfaces to produce $^2O_2^-$ by SPR-assisted electron transfer from Au or Ag to $^3O_2$, which further result in surface metal oxides or hydroxides, as depicted in Equations (2) to (5) (M = Au or Ag).

$$M + h\nu \rightarrow M^* \quad (2)$$

$$^3O_2 + M^* \rightarrow {}^2O_2^- + M^+ \quad (3)$$

$$^2O_2^- + M(M^+) \rightarrow {}^2O_2^- - M(^3O_2 - M \text{ or } ^1O_2 - M) \quad (4)$$

$$^2O_2^- - M(^3O_2 - M \text{ or } ^1O_2 - M)(+H_2O) \rightarrow M_2O(MOH) \quad (5)$$

It has also been pointed out that the local heating effect induced by SPR may play a critical role in the oxidation reaction.[1b,c,2g] Therefore, the heat generated by SPR may also be favorable for the adsorption and dissociation of $^3O_2$.

On the basis of the above results, we depict the elementary steps of the SPR-assisted activation of $^3O_2$ on Au or Ag and its chemical activity in the selective oxidation of PATP in Figure 4. At the beginning, the SPR of the nanoparticles is excited by the laser and results in electron transfer

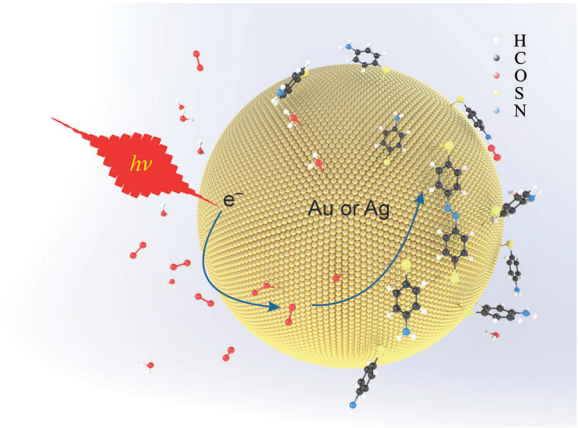

Figure 4. SPR-assisted selective oxidation on the surfaces of Au or Ag nanoparticles (the size of the atoms is present only for visual simplicity and is not to scale).

from nanoparticles to $^3O_2$ in air to yield $^2O_2^-$. Then, $^2O_2^-$ is strongly adsorbed on the surface of the nanoparticles. Meanwhile, because of the oscillation of the free electron under the SPR condition, the local temperature of the nanoparticle surface rises and drives the formation of Au or Ag oxides or hydroxides, which further selectively oxidize PATP to yield DMAB. Besides the selective oxidation of PATP, the SPR-assisted activation of $^3O_2$ and thereafter production of Au or Ag oxides/hydroxides may also play an important role in some other important phenomena, such as the sensitization of $^3O_2$ and the epoxidation of ethylene.[2c,3] The above process depends on the laser wavelength, which affects the efficiency of electron donation and heat generation, and thereby synergistically facilitates the adsorption and dissociation of $^3O_2$ and the production of surface oxides and hydroxides.

In summary, we have scrutinized the mechanism of SPR-assisted activation of $^3O_2$ on Au and Ag nanostructures by monitoring the selective oxidation of PATP to DMAB using SERS. Au, Ag, and Cu have been thought to be inefficient catalysts for many reactions. However, since they are free-electron metals and have a strong SPR effect in the visible-light region, we would expect they will be highly catalytically active after illumination of visible light because of the efficient excitation of the SPR process and the activation of surface processes. It will be particularly important that solar energy can be used to drive such a synthesis by SPR-assisted chemical transformation. For this purpose, we have developed various Au core–transition-metal shell nanoparticles with high catalytic and SPR properties.[11] With these nanoparticles, the SPR properties of the Au core can be used to enhance the catalytic activity of the transition-metal shells. On the other hand, the SPR effect of the Au core can still provide sufficiently strong SERS effect, and the nanoparticles can also serve as ideal signal enhancers to in situ probe the fingerprint information of a SPR-assisted reaction, with strict control of the laser power during Raman measurements. With the aid of this kind of nanoparticles, we expect a new era of SPR-assisted catalytic reactions.

Experimental Section

The Au (ca. 55 nm in diameter), Ag (ca. 80 nm in diameter), and Au core–silica shell (Au@SiO_2) NPs were respectively synthesized according to our previous methods.[12a,b] The Au film (Ag film, Au(111))/PATP/Au (Ag) NP junctions were constructed by assembling PATP and nanoparticles on Au, Ag flat film or Au(111) single crystal using a "layer-by-layer" procedure (see section S4 in the Supporting Information).[12c]

The prepared junctions on Au and Ag films were transferred into a gloves box filled by N_2 where the concentration of $^3O_2$ and water is 0.4 and 0.01 ppm, respectively. Then, the films were tightly sealed between two optical windows. Finally, the sealed films were measured using a Raman microscope. The Raman measurements in NaOH, H_2SO_4, and HCl solutions were performed by dropping these solutions onto Au and Ag nanoparticles dispersed on silicon wafers and preadsorbed with PATP under ambient condition.

Raman spectra were obtained on XploRA (Jobin Yvon-Horiba, France) and Invia (Renishaw, UK) confocal Raman microscopes. Both of the Raman systems are integrated with dark field function. The two systems have a range of lasers of 532 nm (both), 638 nm (XploRA), 632.8 nm (Invia), and 785 nm (both). All the Raman measurements were performed on XploRA except for the wavelength-dependent experiment of Au film/PATP/Au junctions on Invia.

The DFT calculations were carried out with Gaussian 09B.[12d] The full geometry optimization and energy calculation of the ground state and transition state were performed by the hybrid density functional B3LYP. The basis set for S, O, N, C, H were 6-311 + G**. The valence electrons and core electrons of Au and Ag were described by LanL2DZ and its effective core potential.

Received: November 20, 2013
Published online: January 31, 2014

Keywords: nanoparticles · oxygen · oxidation · surface plasmon resonances · surface-enhanced Raman spectroscopy

[1] a) S. Baldelli, A. S. Eppler, E. Anderson, Y.-R. Shen, G. A. Somorjai, *J. Chem. Phys.* **2000**, *113*, 5432–5438; b) S. Eustis, M. A. El-Sayed, *Chem. Soc. Rev.* **2006**, *35*, 209–217; c) S. Lal, N. K. Grady, J. Kundu, C. S. Levin, J. B. Lassiter, N. J. Halas, *Chem. Soc. Rev.* **2008**, *37*, 898–911.

[2] a) L. Brus, *Acc. Chem. Res.* **2008**, *41*, 1742–1749; b) H. Zhu, X. Ke, X. Yang, S. Sarina, H. Liu, *Angew. Chem.* **2010**, *122*, 9851–9855; *Angew. Chem. Int. Ed.* **2010**, *49*, 9657–9661; c) P. Christopher, H. Xin, S. Linic, *Nat. Chem.* **2011**, *3*, 467–472; d) Y. K. Lee, C. H. Jung, J. Park, H. Seo, G. A. Somorjai, J. Y. Park, *Nano Lett.* **2011**, *11*, 4251–4255; e) A. Primo, T. Marino,

A. Corma, R. Molinari, H. García, *J. Am. Chem. Soc.* **2011**, *133*, 6930 – 6933; f) J. Lee, S. Mubeen, X. Ji, G. D. Stucky, M. Moskovits, *Nano Lett.* **2012**, *12*, 5014 – 5019; g) S. Mukherjee, F. Libisch, N. Large, O. Neumann, L. V. Brown, J. Cheng, J. B. Lassiter, E. A. Carter, P. Nordlander, N. J. Halas, *Nano Lett.* **2012**, *12*, 240 – 247; h) S. Mubeen, J. Lee, N. Singh, S. Kramer, G. D. Stucky, M. Moskovits, *Nat. Nanotechnol.* **2013**, *8*, 247 – 251.

[3] a) Y. Zhang, K. Aslan, M. J. R. Previte, C. D. Geddes, *Proc. Natl. Acad. Sci. USA* **2008**, *105*, 1798 – 1802; b) R. Toftegaard, J. Arnbjerg, K. Daasbjerg, P. R. Ogilby, A. Dmitriev, D. S. Sutherland, L. Poulsen, *Angew. Chem.* **2008**, *120*, 6114 – 6116; *Angew. Chem. Int. Ed.* **2008**, *47*, 6025 – 6027; c) R. Vankayala, A. Sagadevan, P. Vijayaraghavan, C. L. Kuo, K. C. Hwang, *Angew. Chem.* **2011**, *123*, 10828 – 10832; *Angew. Chem. Int. Ed.* **2011**, *50*, 10640 – 10644.

[4] a) M. Fleischmann, P. J. Hendra, A. J. McQuillan, *Chem. Phys. Lett.* **1974**, *26*, 163 – 166; b) M. G. Albrecht, J. A. Creighton, *J. Am. Chem. Soc.* **1977**, *99*, 5215 – 5217; c) D. L. Jeanmaire, R. P. Van Duyne, *J. Electroanal. Chem.* **1977**, *84*, 1 – 20; d) S. Nie, S. R. Emory, *Science* **1997**, *275*, 1102 – 1106; e) K. Kneipp, Y. Wang, H. Kneipp, L. T. Perelman, I. Itzkan, R. R. Dasari, M. S. Feld, *Phys. Rev. Lett.* **1997**, *78*, 1667.

[5] C. Pettenkofer, I. Pockrand, A. Otto, *Surf. Sci.* **1983**, *135*, 52 – 64.

[6] a) R. S. Venkatachalam, F. J. Boerio, P. G. Roth, *J. Raman Spectrosc.* **1988**, *19*, 281 – 287; b) N. H. Jang, J. S. Suh, M. Moskovits, *J. Phys. Chem. B* **1997**, *101*, 1649 – 1654; c) A. Kudelski, B. Pettinger, *Chem. Phys. Lett.* **2000**, *321*, 356 – 362; d) D. H. Jeong, J. S. Suh, M. Moskovits, *J. Phys. Chem. B* **2000**, *104*, 7462 – 7467; e) D. Y. Wu, X. M. Liu, Y. F. Huang, B. Ren, X. Xu, Z. Q. Tian, *J. Phys. Chem. C* **2009**, *113*, 18212 – 18222; f) Y. Fang, Y. Li, H. Xu, M. Sun, *Langmuir* **2010**, *26*, 7737 – 7746; g) Y. F. Huang, H. P. Zhu, G. K. Liu, D. Y. Wu, B. Ren, Z. Q. Tian, *J. Am. Chem. Soc.* **2010**, *132*, 9244 – 9246; h) Y. F. Huang, D. Y. Wu, H. P. Zhu, L. B. Zhao, G. K. Liu, B. Ren, Z. Q. Tian, *Phys. Chem. Chem. Phys.* **2012**, *14*, 8485 – 8497; i) M. Sun, H. Xu, *Small* **2012**, *8*, 2777 – 2786; j) E. M. van Schrojenstein Lantman, T. Deckert-Gaudig, A. J. G. Mank, V. Deckert, B. M. Weckhuysen, *Nat. Nanotechnol.* **2012**, *7*, 583 – 586; k) P. Xu, L. Kang, N. H. Mack, K. S. Schanze, X. Han, H.-L. Wang, *Sci. Rep.* **2013**, *50*, DOI: 10.1038/srep02997.

[7] D. Y. Zemlyanov, E. Savinova, A. Scheybal, K. Doblhofer, R. Schlögl, *Surf. Sci.* **1998**, *418*, 441 – 456.

[8] G. K. Liu, J. Hu, P. C. Zheng, G. L. Shen, J. H. Jiang, R. Q. Yu, Y. Cui, B. Ren, *J. Phys. Chem. C* **2008**, *112*, 6499 – 6508.

[9] a) R. Pal, L. M. Wang, Y. Pei, L. S. Wang, X. C. Zeng, *J. Am. Chem. Soc.* **2012**, *134*, 9438 – 9445; b) Z. Luo, G. U. Gamboa, J. C. Smith, A. C. Reber, J. U. Reveles, S. N. Khanna, A. W. Castleman, *J. Am. Chem. Soc.* **2012**, *134*, 18973 – 18978; c) A. P. Woodham, G. Meijer, A. Fielicke, *Angew. Chem.* **2012**, *124*, 4520 – 4523; *Angew. Chem. Int. Ed.* **2012**, *51*, 4444 – 4447.

[10] a) L. L. Zhao, L. Jensen, G. C. Schatz, *J. Am. Chem. Soc.* **2006**, *128*, 2911 – 2919; b) C. M. Aikens, G. C. Schatz, *J. Phys. Chem. A* **2006**, *110*, 13317 – 13324.

[11] Z. Q. Tian, B. Ren, J. F. Li, Z. L. Yang, *Chem. Commun.* **2007**, 3514 – 3534.

[12] a) G. Frens, *Nat. Phys. Sci.* **1973**, *241*, 20 – 22; b) J. F. Li, *et al.*, *Nature* **2010**, *464*, 392 – 395; c) Y. F. Huang, N. N. Yin, X. Wang, D. Y. Wu, B. Ren, Z. Q. Tian, *Chem. Eur. J.* **2010**, *16*, 1449 – 1453; d) M. J. Frisch, et al., Gaussian 09, Revision B.01, Gaussian, Inc., Wallingford CT, **2009**.

